Anisotropy of the Taylor scale and the correlation scale in plasma sheet and solar wind magnetic field fluctuations

James M. Weygand,[1] W. H. Matthaeus,[2] S. Dasso,[3] M. G. Kivelson,[1] L. M. Kistler,[4] and C. Mouikis[4]

[1] Magnetic field data from nine spacecraft in the magnetospheric plasma sheet and the solar wind are employed to determine the correlation scale and the magnetic Taylor microscale from simultaneous multiple-point measurements for multiple intervals with a range of mean magnetic field directions. We have determined that in the solar wind the Taylor scale is independent of direction relative to the mean magnetic field, but the correlation scale along the mean magnetic field ($2.7 \times 10^6 \pm 0.2 \times 10^6$ km) is longer than along the perpendicular direction ($1.5 \times 10^6 \pm 0.1 \times 10^6$ km). Within the plasma sheet we found that the correlation scale varies from $16,400 \pm 1000$ km along the mean magnetic field direction to 9200 ± 600 km in the perpendicular direction. The Taylor scale is also longer parallel to the magnetic field (2900 ± 100 km) than perpendicular to it (1100 ± 100 km). In the solar wind the ratio of the parallel correlation scale to the perpendicular correlation scale is 2.62 ± 0.79; in the plasma sheet the ratio is 1.78 ± 0.16, which indicates that the turbulence in both regions is anisotropic. The correlation and Taylor scales may be used to estimate effective magnetic Reynolds numbers separately for each angular channel. Reynolds numbers were found to be approximately independent of the angle relative to the mean magnetic field. These results may be useful in magnetohydrodynamic modeling of the solar wind and the magnetosphere and can contribute to our understanding of solar and galactic cosmic ray diffusion in the heliosphere.

1. Introduction

[2] In the cascade picture of broad band turbulence, energy resides mainly at large scales, but is transferred across scales by nonlinear processes, eventually reaching small scales where dissipation mechanisms of kinetic origin limit the transfer, dissipate the fluid motions, and deposit heat. This general picture is expected in hydrodynamics and in fluid plasma models such as magnetohydrodynamics (MHD) when the associated Reynolds number and magnetic Reynolds number are large compared to unity, implying that nonlinear couplings are much stronger than the dissipation processes at large scales and that structures having a wide range of spatial scales will be involved in the dynamics. A broadband character is found in fluctuations of the magnetic field (and other quantities such as velocity and density) in the solar wind and in the plasma sheet. Many studies of turbulence in these systems [*Borovsky et al.*, 1997; *Tu and Marsch*, 1995; *Goldstein et al.*, 1995, 1994] analyze the cascade process through spectral analysis or through analysis of structure functions at various orders. Such analysis emphasizes the self-similar range of scale properties that give rise to descriptions such as the famous power law of Kolmogorov theory [*Kolmogorov*, 1941] and its variants [*Kraichnan*, 1965]. In hydrodynamics, the self-similar range is typically defined as extending from an energy-containing scale down to a Kolmogorov dissipation scale. Thus the two most studied length scales are those that define the long wavelength and short wavelength ends of the power law inertial spectral range. The energy-containing scale λ_{CS} is typically of the same order as the correlation scale, which can be computed using classical methods based on the assumption of Taylor frozen-in flow. The dissipation scale L_{diss} in hydrodynamics is the scale at which the turbulent cascade is critically damped and therefore there is significant energy deposited into heat. However, at slightly larger wavelengths ($1/k$) than the dissipation scale, the eddy viscous dissipation time $1/(k^2 \nu)$, where ν is the viscosity,

[1]Institute of Geophysics and Planetary Physics, University of California, Los Angeles, California, USA.
[2]Bartol Research Institute, Department of Physics and Astronomy, University of Delaware, Newark, Delaware, USA.
[3]Instituto de Astronomía y Física del Espacio and Departamento de Física, Universidad de Buenos Aires, Buenos Aires, Argentina.
[4]Experimental Space Plasma Group, University of New Hampshire, Durham, New Hampshire, USA.

becomes equal to the global eddy turnover time λ_{CS}/u (energy per unit mass u^2) signaling the onset of damping of the turbulent eddies in the cascade. The corresponding length λ_T is the Taylor microscale, which also is associated with the mean square gradients of the primitive (velocity) field. (Of the possible definitions of the Taylor scale, which differ mainly by constant factors [*Batchelor*, 1970; *Matthaeus et al.*, 2008], we will choose a form that is simple to implement.) As in earlier work [*Weygand et al.*, 2007; *Matthaeus et al.*, 2008] we take the fundamental definition of Taylor scale to be the length scale associated with the second derivative of the two-point magnetic field correlation function evaluated at zero separation, i.e., the radius of curvature at the origin With these definitions, and the large-scale Reynolds number given as $R = u \lambda_{CS}/\nu$, the Taylor and correlation scales are related by [*Batchelor*, 1970]

$$R_{eff} = \left(\frac{\lambda_{CS}}{\lambda_T}\right)^2 \qquad (1)$$

[3] In the related fields of plasma physics, magnetohydrodynmics and space plasmas, the analysis of turbulence data has proceeded in analogy to the hydrodynamics case, with some differences. The correlation scale is often computed using single point measurements and assuming frozen-in flow when the mean velocity is supersonic and super-Alfvénic, an assumption that introduces some errors. Furthermore, the presence of dispersive waves with possibly high phase velocities makes this procedure subject to additional inaccuracies. Correlation scales can also be computed using the two-point, or two-spacecraft, method outlined by *Matthaeus et al.* [2005]. The upper wave number end of the inertial range, usually seen at ion length kinetic scales in solar wind turbulence, is usually called the dissipation range in keeping with hydrodynamics, even though it may be dispersion that causes the spectrum to steepen. In principle, dissipation processes may contribute only at higher wave number. While it does seem likely that some dissipation is associated with ion scales, in any event it seems clear that the spectral steepening near the ion inertial scale or gyroscale signals the end of the fluid MHD inertial scales. In this way the terminology "dissipation range" remains appropriate in spite of occasional semantic confusion. Finally the analogs of the Taylor microscale in space plasmas have been almost completely ignored prior to this time, mainly because of instrumental limitations. Like the correlation scale, the Taylor scale can be determined from cross correlations and the details of this method are outlined by *Weygand et al.* [2007].

[4] Turbulence in the solar wind is thought to originate at least in part in the source regions of the solar atmosphere, where it is the product of coronal dynamical processes. Solar wind turbulence may also be driven by stream interactions, including compressions and shears, which are almost certainly responsible for augmentation of turbulence seen at 1 AU and beyond, as well as the disappearance of Alfvénic correlations with increasing heliocentric distance [*Roberts et al.*, 1987]. These drivers may also be responsible for the heating that underlies the observed highly nonadiabatic temperature profile that extends from inside 1 AU to beyond 60 AU as observed by Voyager and Pioneer [*Gazis et al.*, 1994; *Richardson et al.*, 1995; *Williams et al.*, 1995; *Smith et al.*, 2001].

[5] Solar wind turbulence is modified by the anisotropy resulting from the presence of a large-scale magnetic field that affects the propagation and acceleration of cosmic rays [*Duffy and Blundell*, 2005] and the heating of the interplanetary plasma [*Velli*, 2003]. These anisotropic fluctuations have been analyzed using both the slab model and the "2-D" model. In the slab model, the wave vectors consist of Alfvén waves that are aligned with and propagate along the mean magnetic field. The correlation function for this model has the shortest scales parallel to the mean magnetic field and the longest scale in the perpendicular direction [*Dasso et al.*, 2005; *Osman and Horbury*, 2007]. Unfortunately, this model does not allow for incompressible mode coupling and thus cannot produce a turbulent Kolmogorov-like cascade [*Oughton and Matthaeus*, 2005]. In the 2-D model the excited wave vectors and magnetic field fluctuations lie in the plane perpendicular to the mean magnetic field; the correlation function has the shortest scales in the perpendicular direction and longer scales in the parallel direction [*Dasso et al.*, 2005; *Osman and Horbury*, 2007]. A superposition of slab and 2-D fluctuations forms a convenient parameterized model for anisotropy that has been employed for convenience in a variety of applications [e.g., *Bieber et al.*, 1994].

[6] To characterize the anisotropy in observations directly without using the frozen-in approximation, simultaneous two point measurements of the turbulence fluctuations at a variety of angles relative to the mean magnetic field direction are required. Because such measurements were not previously available, indirect measurement of anisotropy has been attempted in numerous studies, using single spacecraft data. For example, in one early study, *Matthaeus et al.* [1990] employed magnetic field fluctuations measured by ISEE 3 in the solar wind, and found an anisotropic correlation function with a "Maltese cross" shape. They interpreted this shape to be the result of a superposition of slab and 2-D fluctuations. *Bieber et al.* [1996] examined the ratio of the perpendicular and quasi-parallel spectra, along with the dependence of the total power spectrum on the angle between the mean magnetic field and the solar wind flow direction, to measure the relative amplitudes of the slab and two-dimensional power. They found that about 85% of the energy was in the 2-D component. The study of *Dasso et al.* [2005], using autocorrelation measurements from a single spacecraft, took the work of *Matthaeus et al.* [1990] one step further by subdividing the solar wind magnetic field and plasma flow data into fast (>500 km/s) and slow (<400 km/s) solar wind intervals. In both the magnetic field and flow data, they found that quasi two-dimensional fluctuations dominate in the slow solar wind and slab fluctuations are more prominent in the fast solar wind. In a recent solar wind study, *Osman and Horbury* [2007] used multispacecraft time-lagged two-point correlation measurements obtained by the Cluster mission to construct a spatial autocorrelation function. They demonstrated that the solar wind fluctuations are anisotropic by showing that the ratio of the correlation length along the magnetic field to the perpendicular correlation length is 1.79 ± 0.36. From numerical simulations of incompressible, three-dimensional, MHD turbulence, *Milano et al.* [2001] found that the

correlation scale along the locally averaged magnetic field direction is larger than along direction perpendicular to the local mean magnetic field. The fact that the correlations are longest along the magnetic field suggests that the solar wind includes a substantial ingredient of quasi-2-D fluctuations, for which a leading order description is the 2-D model.

[7] The magnetospheric plasma sheet has also revealed properties associated with turbulence. Electromagnetic energy is stored in the magnetotail lobes from which it is transferred to the plasma sheet, producing flows and heating the plasma; the dominant mechanism for this transport is most likely reconnection. As a consequence, fluctuations of plasma sheet flows have a disordered appearance [*Borovsky et al.*, 1997; *Weygand et al.*, 2005, 2006]. Understanding these fluctuations is important for understanding the role of turbulence in the transport of lobe electromagnetic energy and mass to the plasma sheet. However, measurements to ascertain the role of plasma sheet turbulence in energy transport remain incomplete. A key characteristic of plasma sheet turbulence that has not yet been studied is the dependence of the scale sizes of the turbulent energy cascade on the direction of the mean magnetic field. This study addresses that matter using multispacecraft correlations to examine the anisotropy of the turbulent fluctuations.

[8] In previous papers we presented preliminary results on the correlation scale and the Taylor scale in solar wind and plasma sheet turbulence using simultaneous two point measurements acquired by pairs of interplanetary spacecraft [*Matthaeus et al.*, 2005; *Weygand et al.*, 2007]. The correlation scale from the *Matthaeus et al.* [2005] study was determined from a robust fit of an exponential function to the data. The Taylor scale in the *Weygand et al.* [2007] study was determined from a new method based on the Richardson extrapolation technique. The approach here is similar; however we have now accumulated two-spacecraft samples in sufficient numbers to resolve the correlations into angular bins relative to the locally computed mean magnetic field. This makes possible a two-spacecraft study of anisotropy, which is the emphasis of the present paper.

[9] In the following sections we refer to the above mentioned references for methodological details. We will use our augmented database of two spacecraft correlation data to determine, in both the interplanetary plasma and the plasma sheet, the Taylor scale (λ_T) and the correlation scale (λ_{CS}). Each type of measurement will be resolved in angular channels to describe anisotropy relative to the mean magnetic field. We will also derive quantitative estimates of the effective magnetic Reynolds number. Finally, we compare the present results with previously published estimates based on single-spacecraft and multispacecraft observations of the associated scales.

2. Instrumentation

[10] For this study the magnetic field measurements taken within the plasma sheet and solar wind were obtained from many different spacecraft. Measurements in the solar wind were obtained from the Cluster, ACE, Geotail, IMP 8, Interball, and Wind. For the plasma sheet, measurements were recorded by Cluster, Geotail, and Wind. This large number of spacecraft provides effectively simultaneous two-point plasma and field measurements at a large range

of spatial separations, enabling us to measure spatial correlations as a function of separation directly instead of inferring them by interpreting temporal fluctuations as frozen into a flowing plasma [*Taylor*, 1938].

[11] The Cluster mission, supported jointly by the European Space Agency (ESA) and National Aeronautics and Space Administration (NASA), consists of four identical spacecraft, optimally in a tetrahedral configuration, with a perigee of 4 R$_E$, an apogee of 19.6 R$_E$, and a spin period of about 4 s. These four spacecraft provide the first three-dimensional measurements of large- and small-scale phenomena in the near-Earth environment [*Escoubet et al.*, 1997]. Each Cluster spacecraft carries 11 instruments. This study uses data from the magnetometer (FGM) [*Balogh et al.*, 1997] and the ion spectrometer (CIS) [*Rème et al.*, 1997]. The Cluster apogee precesses around the Earth annually. From 2001 to 2007, between July and October the Cluster spacecraft apogees were in the magnetotail and between January and April they were intermittently in the solar wind. At apogee in the summer seasons the spacecraft were located at the vertices of nearly regular tetrahedrons. The scales of the tetrahedral differed from one season to the next, covering a range of distances pertinent to turbulence studies. In the magnetotail seasons of 2001 and 2004, the tetrahedron's scale was about 1000 km, which is close to the short wavelength limit of the inertial range. During the 2002 season the scale was 5000 km (i.e., on the order of the inertial range for turbulence within the plasma sheet). The latter spacing is ideal for examining turbulent eddy scale sizes that are well within the inertial range [*Neagu et al.*, 2002; *Weygand et al.*, 2005]. From July to October 2003, Cluster obtained another series of plasma sheet crossings at an interspacecraft spacing of about 100 km (i.e., on the order of dissipation range). In the magnetotail seasons of 2005 and 2006 the tetrahedral formation was not used; instead two pairs of spacecraft were separated by about 10,000 km and the separation within a pair was 1000 km.

[12] Each Cluster spacecraft carries a boom-mounted triaxial fluxgate magnetometer [*Balogh et al.*, 1997]. Magnetic field vectors routinely are available at 22 Hz resolution (nominal mode). Both preflight and in-flight calibrations of the two magnetometers have been performed to produce carefully calibrated (and intercalibrated) magnetic field data. The relative uncertainty in the data after calibration is at most 0.1 nT, an estimate determined by examining the drift in the offset after calibration (K. K. Khurana and H. Schwarzl, private communication, 2004). The digital resolution of the magnetometer is on the order of 8 pT [*Balogh et al.*, 1997].

[13] Data from the CIS instrument [*Rème et al.*, 1997], along with the magnetic field data, are essential in identifying periods when Cluster enters the plasma sheet and when it is in the solar wind. CIS provides fundamental plasma parameters such as density, velocity vectors, the pressure tensor, and heat flux. The uncertainties in most of these quantities are not significant for this study. Entry and exit from the plasma sheet are identified from significant increases or decreases of the density and ion temperature. Although plasma data not are available from all four spacecraft, intervals in the solar wind or the plasma sheet can be established from the available measurements because the spacecraft are close to one another.

Table 1. Solar Wind and Plasma Sheet Spacecraft Pairs

Spacecraft Pair	Interval of Spacecraft Pair	Potential Separations (km)
ACE-Geotail	Feb 1998 to Jun 2004	$1.26 \cdot 10^6$ to $1.57 \cdot 10^6$
ACE-Wind	Feb 1998 to Jun 2004	$0.14 \cdot 10^6$ to $2.19 \cdot 10^6$
Geotail-IMP 8	Oct 1994 to Oct 1999	$0.74 \cdot 10^5$ to $9.20 \cdot 10^5$
Geotail-Interball	Apr 1996 to Jul 1999	$0.68 \cdot 10^5$ to $2.80 \cdot 10^5$
Geotail-Wind	Aug 1995 to Aug 2006	$0.13 \cdot 10^6$ to $1.63 \cdot 10^6$
Cluster 1, 2, 3, and 4	Feb 2001 to Oct 2007	$0.08 \cdot 10^3$ to $20.0 \cdot 10^3$

[14] In addition to Cluster data, we also use solar wind data from the ACE, Geotail, IMP 8, Interball, and Wind spacecraft. On all five of these spacecraft we use data from triaxial fluxgate magnetometers [*Smith et al.*, 1998; *Kokubun et al.*, 1994; *Nozdrachev et al.*, 1995; *Lepping et al.*, 1995] to obtain the local IMF direction and magnitude at temporal resolution ranging from 3 s to 16 s.

3. Procedure and Observations

[15] The intervals used in this study are obtained from two distinct regions: the solar wind and the plasma sheet. For each plasma region, data selection criteria are specified. The solar wind data intervals are selected visually from plotted data by excluding data corresponding to the bow shock or the magnetosheath. The solar wind is identified from the magnetic field data, which had typical magnitudes of around 5 to 10 nT, the plasma density, which was of the order of several particles per cm^{-3}, and the solar wind speed, which was less than or equal to 450 km s^{-1}. The choice of 450 km s^{-1}, although arbitrary, is characteristic of the break between the two types of solar wind. We do not use solar wind data with sharp rotations in the IMF B_x and B_y components in order to exclude sector boundary crossings. We also exclude solar wind shocks. In order to obtain meaningful cross-correlation coefficients, we require over 12 h of continuous data at 1 min resolution from the ACE, Geotail, IMP 8, Interball, and Wind spacecraft. We interpolated the data to 1 min resolution in order to obtain simultaneous field vectors at different spatial locations. The Cluster spacecraft remain relatively close together and were used to characterize fluctuations over short distances. Because they do not remain in the solar wind for long periods, we relaxed the condition on interval length, requiring only 1 h or more of solar wind data from Cluster. The Cluster orbit remained in relatively close proximity to the magnetosphere, even when in the solar wind. Inevitably we include some measurements in which foreshock waves were present in the solar wind. To minimize the contribution of such waves to our analysis, the solar wind magnetic field measurements are averaged to 30 s resolution, which is approximately the longest period for ion foreshock waves. As an additional check we have examined a subset of solar wind intervals when there are no foreshock waves or shocklets and found that the results are similar to those in the full data set.

[16] For the plasma sheet analysis, we require at least 1 h of continuous 4 s average magnetic field data. Entries and exits from the plasma sheet as identified as times when the ion temperature significantly increases or decreases. Within the plasma sheet we require the ion density to be greater than 0.1 cm^{-3} and the magnetic field B_x component to have

values between -25 and 25 nT, eliminating intervals during which the spacecraft appear to enter lobe regions owing to magnetotail flapping or other phenomena. For the plasma sheet data analysis we also remove a background magnetic field determined with a cubic fit to the entire data interval. This step is necessary because we are interested in the turbulent magnetic fluctuations and the large-scale structure of the magnetotail field influences the cross-correlation values. Furthermore, we excise intervals at the very center of the plasma sheet ($|\mathbf{B}|$ between -10 and 10 nT) because in this region the magnetic field has a small radius of curvature and the mean magnetic field direction is meaningless.

[17] In order to establish how the average correlation and Taylor scale values depend on the angle relative to the background field, we combine many different solar wind (plasma sheet) intervals. Most of the angular bins for this study are 10° wide but, because there were few intervals in which the spacecraft separation was close to the direction of the background field, we define one bin of 30° width (0° to 30°). In the plasma sheet, the correlation scale is calculated to be the decay length of an exponential obtained from a robust fit to all the cross-correlation coefficients at different spacecraft separations within one angular bin. In the solar wind the correlation scale is determined by fitting the sum of two exponentials to the correlation versus spacecraft separation. Two exponentials were used because a single exponential function produced a poor fit to the data in each angular bin. The Taylor scale is found using a method based on the Richardson extrapolation technique [*Weygand et al.*, 2007]. The Taylor scale is obtained from a set of parabolic fits to the cross-correlation values up to separations that are increased systematically until the Taylor scale values become stable.

3.1. Solar Wind Procedure

[18] For each selected data interval, we calculate the time-averaged cross correlation of the magnetic field vector for each of the spacecraft pairs. This correlation value is assigned to a separation distance, which is the time average of the corresponding spacecraft separation distances for that interval. Each correlation estimate is normalized by the vector variance of the magnetic field fluctuation in the interval [*Matthaeus et al.*, 2005]. By collecting normalized correlation values from a large number of suitable solar wind intervals, we find estimates of the variation of the correlation function with spatial separation, r. Table 1 lists the spacecraft pairs that are used in the solar wind analysis of the present study, along with time ranges within which intervals were selected, and approximate spatial separations.

[19] Figure 1 displays the correlation function for all the spacecraft pairs in the slow solar wind. The spacecraft separations less than 20,000 km are Cluster spacecraft pairs. Spacecraft separations larger than 50,000 km combine measurements from ACE, Geotail, IMP 8, Interball, and Wind. This plot demonstrates that we have a large number of small spacecraft separations, useful for estimating the Taylor scale, and a significant number of data points useful for determining the correlation scale. The absence of spacecraft separations between 20,000 km and 50,000 km does not prevent our estimating the correlation scale because there a significant number of data points on either side of this gap.

Solar Wind Correlation Function
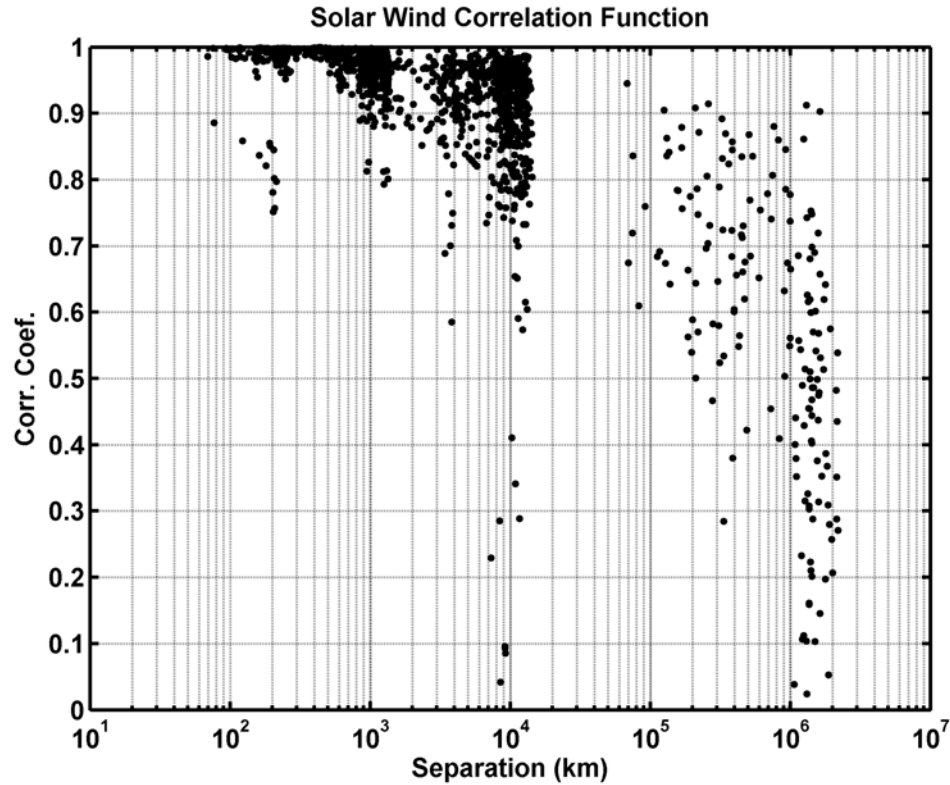
Figure 1. Slow solar wind spacecraft separation versus cross-correlation coefficients for all spacecraft in this study. The separations less than 20,000 km are Cluster spacecraft pairs. Separations above 50,000 km are for all other spacecraft.

[20] For all the solar wind data we determined the absolute value of the spacecraft separation along the perpendicular (x axis) and parallel (y axis) directions with respect to the mean magnetic field and binned the data into angular bins as noted. For each case the mean magnetic field is computed by averaging over the interval. Figure 2 shows the distribution of the data into the different bins. Dashed lines delineate the bin sizes and color is used to show clearly the number of points falling into the different bins. The limited data for spacecraft separations close to the mean magnetic field direction is evident. The lack of measurements along the mean magnetic field is most likely the result of the orbits of the spacecraft and the tendency of the IMF to lie at about 45° in the ecliptic plane with respect to the Sun-Earth line due to the "garden hose" effect.

[21] Figure 3 displays a correlation contour plot for the slow solar wind data. The color bar on the right shows the correlation value for each contour and the perpendicular and parallel separations are along the x and y axis, respectively. It is apparent that the longest correlations are along the mean magnetic field line direction and the shortest correlations are in the perpendicular direction.

[22] Table 2 gives the correlation scale (third column), the Taylor scale (sixth column), and the effective magnetic Reynolds number (last column) for each angular bin. The fourth column contains the second correlation scale determined from the sum of two exponentials fit. The uncertainties of the correlation scale have been determined from the residuals from the robust fit of the exponential function to the cross-correlation values and the uncertainties of the

Taylor scale have been determined from the Richardson extrapolation method discussed by *Weygand et al.* [2007]. The effective magnetic Reynolds numbers are calculated using equation (1) and the uncertainty has been propagated through. Despite differing by an order of magnitude, within the uncertainty nearly all the effective magnetic Reynolds numbers are the same.

[23] Another important feature of this analysis is the determination of correlation lengths in the various angular channels. The summary of this analysis shown in Table 2 shows that the anisotropy of solar wind turbulent fluctuations have anisotropic correlation lengths, with the ratio of the parallel to perpendicular correlation scales found to be 2.62 ± 0.79.

[24] There is some suggestion of variation of correlation scales in the angular channels extending from 30 degrees to 90 degrees from the mean field direction, as values range from $5.6 \cdot 10^6$ km to $2.1 \cdot 10^6$ km, the error bars being somewhat smaller than this variation. However, the parallel channel, from 0° to 30°, has a significantly larger correlation scale of $5.6 \cdot 10^6$ km.

3.2. Plasma Sheet Observations

[25] For the plasma sheet we apply the same techniques for determining the Taylor scale and the effective magnetic Reynolds number from magnetic field data. The correlation scale for the plasma sheet is determined from a single exponential fit to the data. Most of our correlation values are obtained from Cluster spacecraft pairs in regions above or below the central plasma sheet where the mean magnetic
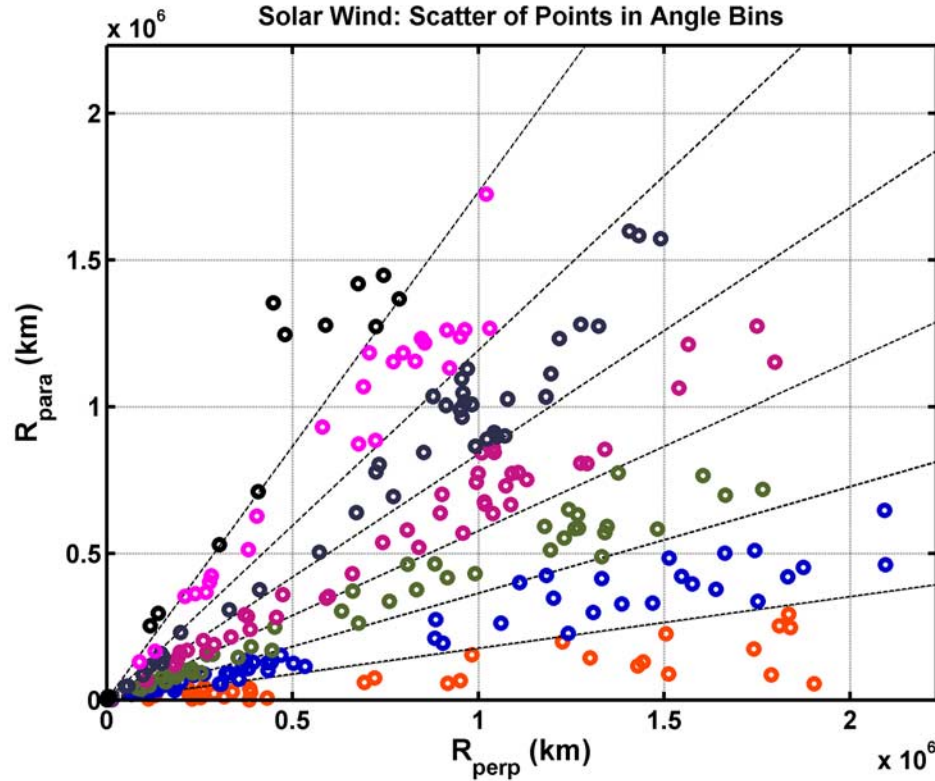
Figure 2. Distribution of spacecraft separations in the parallel and perpendicular directions with respect to the mean magnetic field direction for the slow solar wind. The dashed lines show bin boundaries, and color identifies the points within each bin.

field is relatively straight. Figure 4 displays the correlation versus spacecraft separation for the plasma sheet in the format of Figure 1. We are also fortunate to have some cross-correlation values from Geotail and Wind spacecraft pairs. These points demonstrate that the correlation function approaches zero for separations of 100,000 km.

[26] Figure 5 displays the distribution of the correlation values as a function of the angle relative to the magnetic field direction in the format of Figure 2. There are considerably more data points in the 0° to 30° than in the solar wind analysis; however, the counting statistics are still relatively low. Figure 6 shows the calculated correlation contours in the format of Figure 3. The contours indicate that the correlation length is longest along the mean magnetic field and shortest perpendicular to it. This feature is similar to what was found above for the solar wind case.

[27] Table 3 lists the correlation scale (third column), Taylor scale (fifth column), and the effective magnetic Reynolds number (last column) for each of the angular bins in Figure 5. The uncertainties are determined with the same methods indicated for Table 2. A comparison of the effective magnetic Reynolds number shows that there is considerable scatter in the values. However, a Reynolds number of approximately 45 fits the tabulated values with their uncertainty for all angles. Furthermore Figure 6 and Table 3 show that the correlation scale decreases systematically from the parallel to the perpendicular direction.

[28] The analysis of plasma sheet fluctuations also shows that anisotropy is found in the computed correlation scales. From the data shown, we determine that the ratio of the

parallel to perpendicular correlation scale is 1.78 ± 0.16. This is similar to the analogous result found above for the solar wind.

4. Discussion

4.1. Solar Wind

[29] In section 3 we showed that the correlation scale is longest along the mean magnetic field direction and shortest in the perpendicular direction in both the slow solar wind and the plasma sheet. In the solar wind this result supports the work of *Dasso et al.* [2005] and *Osman and Horbury* [2007]. However, our slow solar wind result disagrees with the data and modeling work shown by *Matthaeus et al.* [1990] and *Crooker et al.* [1982]. *Matthaeus et al.* [1990] calculated two-dimensional wave number power spectra from two-dimensional incompressible MHD simulations and the contours of correlation from single spacecraft autocorrelations of the magnetic field data. They use the solar wind speed and the temporal separation associated with the autocorrelation value to obtain spatial separation. To get the separation in the perpendicular and parallel directions *Matthaeus et al.* [1990] calculate the angle between the mean magnetic field direction and the solar wind flow and they assume that the solar wind flows radially. A ratio of the parallel to perpendicular scale was not given in that study, but a rough estimate of the ratio from Figure 3 of *Matthaeus et al.* [1990] suggests that the ratio is about 0.9. We should note that this earlier study did not employ variance normalization in accumulating results
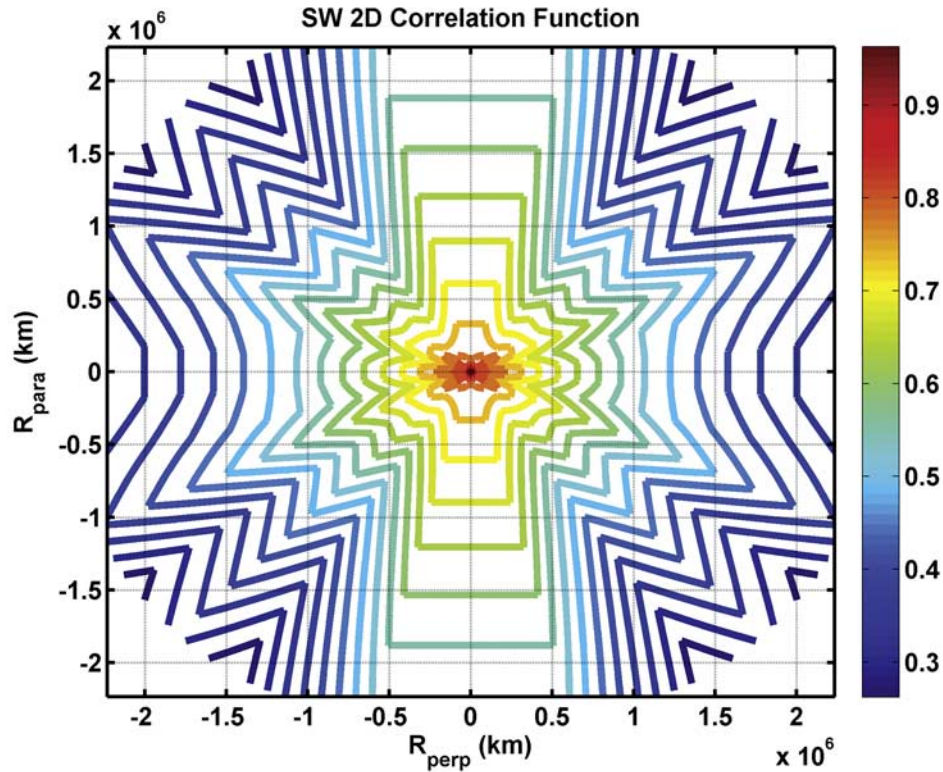
Figure 3. Correlation contour plot for the slow solar wind. The contours are calculated for one quadrant and then mirrored into the other quadrants. The color bar indicates the value of the correlation coefficient. The plot shows that the longest correlations are along the magnetic field direction and the shortest correlation are perpendicular to the magnetic field direction.

from different time intervals of data. This difference, as well as their use of single spacecraft data and frozen-in flow, and the fact that intervals were not separated according to solar wind speed, may account for the considerable difference between their results and the present determination of parallel and perpendicular correlation scales.

[30] *Crooker et al.* [1982] use ISEE 1 and ISEE 3 solar wind data to determine autocorrelation lengths along the IMF and perpendicular to the magnetic field. Like *Matthaeus et al.* [1990], they found the longest correlation lengths perpendicular to the magnetic field (100 to 150 R_E) and the shortest parallel to the magnetic field (50 to 100 R_E). Their study appears to have included both slow and fast solar wind, but the bulk of the measurements were taken in the slow solar wind.

[31] *Dasso et al.* [2005] showed that the anisotropy in the solar wind turbulence differs in the fast and slow solar wind. They found that the fast solar wind contains mainly slab-like turbulence and the slow solar wind contains mostly two-dimensional turbulence. Unfortunately, there were too few two-spacecraft data intervals in the fast solar wind to enable us to compare our multispacecraft correlation contours to those of *Dasso et al.* [2005]. When we compare our slow solar wind correlation contours to their slow solar wind contours (see their Figure 1) we find that the shapes are very similar. *Dasso et al.* [2005] determined a ratio of the parallel to perpendicular correlation scales in the slow solar wind and found a value of 1.2 for the magnetic field fluctuations, which indicates that the slow solar wind turbulence is anisotropic. Their value differs significantly

Table 2. Slow Solar Wind Values of the Correlation Scale, the Taylor Scale, and the Effective Magnetic Reynolds Number Computed From Magnetic Field Data[a]

Angular Range	Correlation Scale			Taylor Scale		
	Number of Points	λ_{CS} (10^6 km)	λ_2 (10^3 km)	Number of Points	λ_{TS} (km)	Effective Magnetic Reynolds Number $\times 10^6$
$0° - 30°$	345	5.6 ± 1.6	24.1 ± 7.6	21	930 ± 160	37.0 ± 35.5
$30° - 40°$	190	2.0 ± 0.3	14.5 ± 7.1	12	1200 ± 620	$2.6. \pm 3.0$
$40° - 50°$	267	2.7 ± 0.4	13.9 ± 5.1	28	700 ± 180	14.8 ± 13.2
$50° - 60°$	345	2.0 ± 0.2	4.1 ± 2.2	52	1400 ± 230	2.0 ± 1.5
$60° - 70°$	399	3.2 ± 0.4	12.4 ± 3.0	50	740 ± 210	18.9 ± 17.3
$70° - 80°$	413	2.9 ± 0.4	13.8 ± 2.9	50	1000 ± 200	8.6 ± 7.1
$80° - 90°$	439	2.1 ± 0.2	3.7 ± 1.1	48	1030 ± 290	4.4 ± 3.8

[a]Also given is the number of points that went into the determination of the correlation scale and Taylor scale values.
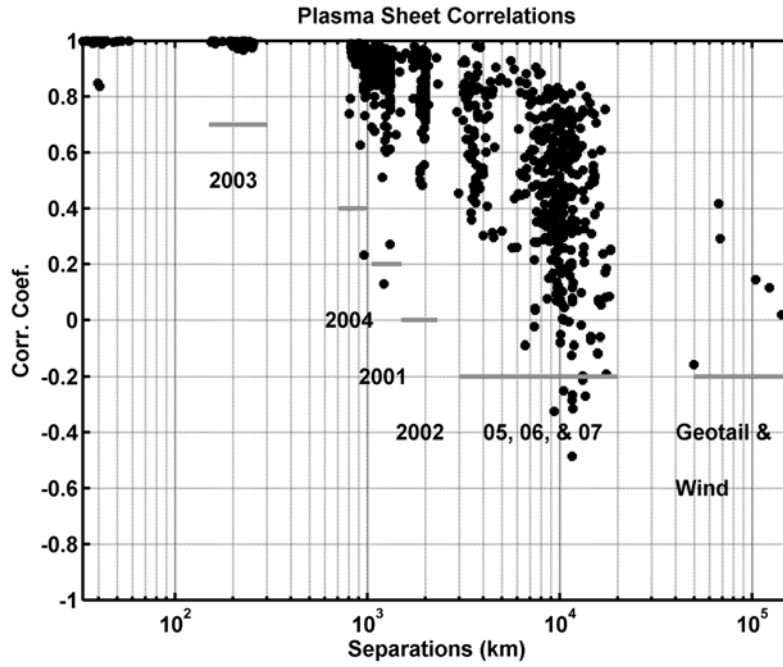
Figure 4. Spacecraft separation versus cross-correlation coefficients for the plasma sheet. Data with separations less than 20,000 km are from the Cluster spacecraft. We have indicated the years of the plasma sheet seasons for the approximate spacecraft separations. Larger separations were obtained from Geotail and Wind spacecraft pairs.
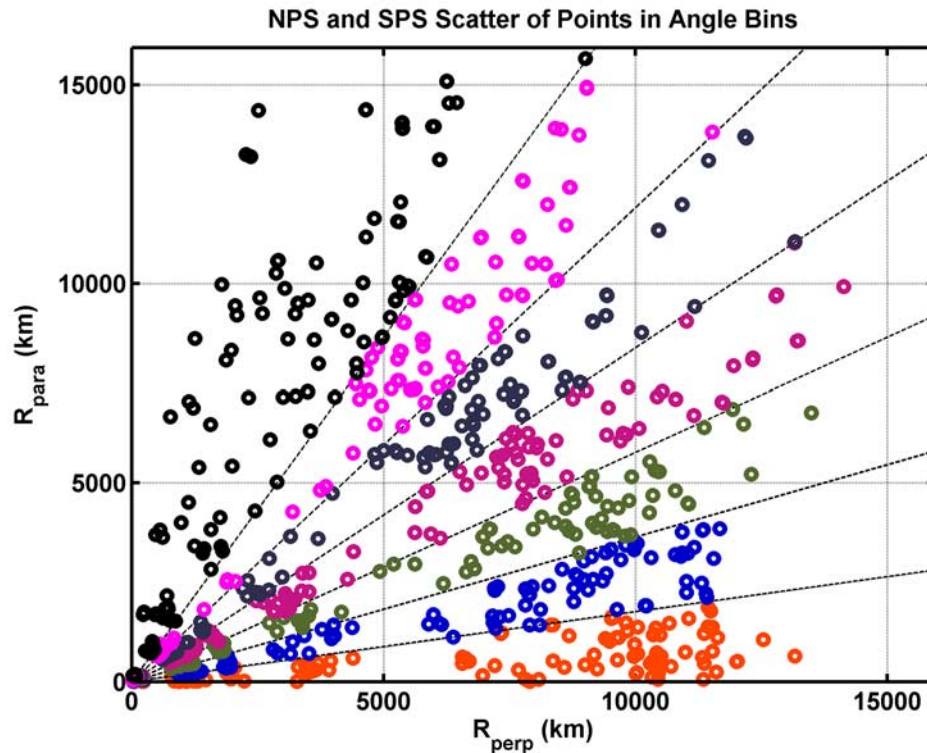
Figure 5. Distribution of spacecraft separations in the parallel and perpendicular directions with respect to the mean magnetic field direction for the plasma sheet. Same format as Figure 2.
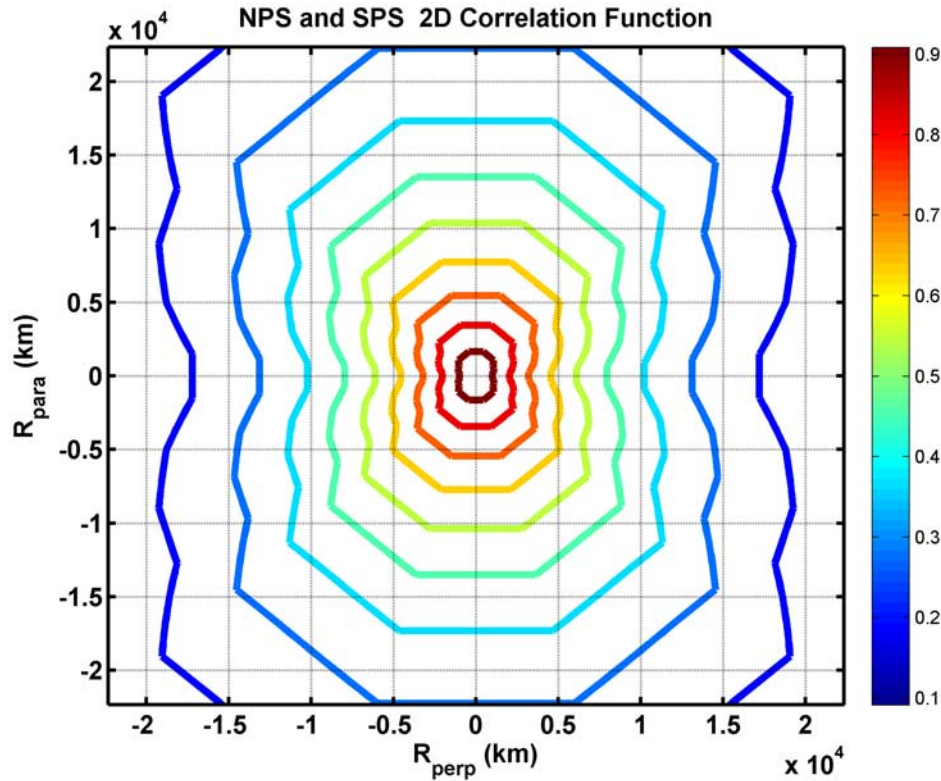
Figure 6. Correlation contour plot for the plasma sheet. Same format as Figure 3. This plot shows that the longest correlations are along the mean magnetic field direction and the shortest correlations are in the perpendicular direction.

from the ratio of 2.62 ± 0.79 found in our study. Possible reasons for this difference are, again, that this earlier study employed single spacecraft data and frozen-in flow, and also that the range of solar wind speeds differs in the two studies. We have limited our analysis to speeds below 450 km s^{-1} whereas *Dasso et al.* [2005] included only speeds below 400 km s^{-1}. However, we would have expected the anisotropy to increase for lower solar wind speeds if the two different types of turbulence are speed dependent (i.e., dependent on their origin in the solar atmosphere). We have reanalyzed our results using solar wind speeds below 400 km s^{-1}, but with larger angular bins (30°) because of the limited number of events available. With this restricted range of solar wind speeds, the ratio of the parallel to perpendicular correlation scales is 1.27 ± 0.35, in agreement with the results of *Dasso et al.* [2005] within the uncertainty. This marked change in the anisotropy for a change of only 50 km/s in the cutoff velocity may suggest that the

anisotropy depends strongly on solar wind speed, but the difference may also be related to the larger angular bins used to obtain the new ratio. When the anisotropy ratio is recalculated for solar wind speed less than 450 km s^{-1} with larger 30° angular bins, then the ratio becomes 2.11 ± 0.63, which overlaps with the uncertainty of the ratio for flows less than 400 km s^{-1}. This smaller value suggests that the angular bin size does play a role in producing lower anisotropy ratios.

[32] The study most similar to ours is that of *Osman and Horbury* [2007]. That study constructed a spatial autocorrelation function by using time-lagged two-point correlations obtained from the x and the z components of the Cluster magnetic field data in the solar wind during a slow solar wind interval. They also found that the parallel correlation scale was longest along the mean magnetic field direction and the mean ratio of the parallel to perpendicular correlation scale for all three components of the magnetic

Table 3. Plasma Sheet Values of Correlation Scale, Taylor Scale, and Effective Magnetic Reynolds Number for the Various Angular Bins From Magnetic Field Data

Angular Range	Correlation Scale		Taylor Scale		Effective Magnetic Reynolds Number
	Number of Points	λ_{CS} (km)	Number of Points	λ_{TS} (km)	
0° − 30°	114	16400 ± 1000	31	2900 ± 100	30 ± 17
30° − 40°	75	14100 ± 1300	6	1700 ± 200	88 ± 59
40° − 50°	98	14800 ± 1200	19	1500 ± 200	97 ± 53
50° − 60°	114	11100 ± 700	42	2200 ± 200	28 ± 17
60° − 70°	141	10600 ± 700	51	1800 ± 100	44 ± 31
70° − 80°	154	10600 ± 600	44	1700 ± 100	50 ± 25
80° − 90°	153	9200 ± 600	48	1100 ± 100	59 ± 47

Table 4. Taylor Scale Determined for Several Angular Bins for Both the Solar and Fast Solar Wind

Angular Bin Range	Slow Solar Wind Taylor Scale (km)	Fast Solar Wind Taylor Scale (km)
0° to 30°	930 ± 160	2300 ± 200
30° to 60°	660 ± 370	1300 ± 80
60 °to 90°	820 ± 250	1300 ± 40

field was 1.79 ± 0.36, which is similar to our value of 2.62 ± 0.79. A ratio of approximately 2 fits the two values with their uncertainty. The *Osman and Horbury* [2007] result employs an interesting hybrid methodology that uses two-spacecraft data along with a generalization of the frozen-in flow approximation. The present result employs only simultaneous two-spacecraft correlations. The correspondence of these results is of significance, in part because it validates the *Osman and Horbury* [2007] method.

[33] *Matthaeus et al.* [2005, 2008] and *Weygand et al.* [2007] determined the mean correlation and Taylor scale for the solar wind independent of the relative orientation of spacecraft separation and the magnetic field. Here we have considered how these parameters vary as a function of the angle between the spacecraft separation vector and the mean magnetic field direction. We would expect that the average over all the angular bins of the correlation and Taylor scale values with our regard to the number of samples per angular channel would be approximately equal to the mean correlation and Taylor scale values of *Matthaeus et al.* [2005] and *Weygand et al.* [2007]. This average is close for the correlation scale, but there is a difference of approximately a factor of 2. *Matthaeus et al.* [2005] reported a value of about $1.23 \cdot 10^6$ km, while here we find a mean correlation scale value of $2.92 \cdot 10^6 \pm 1.3 \cdot 10^6$ km. This difference is most likely due to the sum of two exponentials fitting function used in this study. However, the angle-averaged Taylor scale does not yield that found in earlier work. *Weygand et al.* [2007] gave a value of 2400 ± 100 km, while the mean value in this study is 1000 ± 200 km. The source of this difference is unclear, but may relate to the fact that *Weygand et al.* [2007] combined slow and fast solar wind data but in this study considers just slow solar wind.

[34] There is enough fast solar wind data with small spacecraft separations to determine the Taylor scale values within 30° angular bins. Table 4 displays the Taylor scale values for three 30° angular bins in both the slow solar wind and fast solar wind, where the fast solar wind is defined as solar wind speeds greater than 500 km/s. The Taylor scale values for the fast solar wind are always larger (by at least a factor of 1.6) than the Taylor scale values for the slow solar wind. These results suggest that there is some difference in character of the turbulence, and possibly the nature of the dissipation processes for the two solar wind regimes. In particular, *Matthaeus et al.* [2008] found some evidence for variation of solar wind magnetic Taylor scale with plasma beta, which may differ in the two types of solar wind.

[35] An alternative definition of the magnetic Taylor microscale is given by *Weygand et al.* [2007]:

$$\lambda_T = \sqrt{\langle b^2 \rangle / \left\langle (\nabla \times \mathbf{b})^2 \right\rangle} \qquad (2)$$

where $\mathbf{b} = \mathbf{B} - \mathbf{B}_0$ is the fluctuation of the total magnetic field, $\mathbf{B}$ is the magnetic field vector, and $\mathbf{B}_0 = \langle \mathbf{B} \rangle$ is the mean magnetic field. It is clear from this definition that λ_T is a length associated with the mean square spatial derivatives of $\mathbf{b}$ [*Batchelor*, 1970]. The data of our study can be used to compare the amplitude of the magnetic field fluctuations of the fast and the slow solar wind. Their amplitudes differ little. The fact that the Taylor scale differs in the two types of solar wind suggests that there is a difference in the currents ($\propto \nabla \times \mathbf{b}$) driving the fluctuations in the two solar wind regimes.

[36] The Taylor scale can also be expressed in terms of the fluctuation spectrum through the relation

$$(1/\lambda_T)^2 = \int_0^\infty d^3k \, k^2 E(\mathsf{k}) / \int_0^\infty d^3k \, E(\mathsf{k}) \qquad (3)$$

where the denominator on the right hand side is the total fluctuation energy. This form makes the sensitivity of the Taylor scale to the steepness of the spectrum particularly evident, since the omnidirectional spectrum

$$E(\mathsf{k}) = k^2 \int d\Omega E(\mathsf{k}), \qquad (4)$$

where $d\Omega$ is the solid angle, must fall off faster than $1/k^3$ for the integral to exist. Recently, P. J. M. Chuychai et al. (Technique of measuring and correcting the Taylor microscale, manuscript in preparation, 2009) demonstrated with empirical models of the correlation functions that the Taylor scale varies with the steepness of the spectrum in the dissipation range and, as the spectral index becomes more negative, the Taylor scale value systematically increases. This study suggests the possibility that slower solar wind intervals have a steeper dissipation range magnetic spectrum. While this question appears not to have been investigated yet, it would help explain how the smaller Taylor scale values found in this study of the slow solar wind (Table 2) would emerge by excluding fast solar wind intervals. This hypothesis is supported by the differences observed in the Taylor scale values given in Table 4.

[37] We used equation (1) to calculate the effective magnetic Reynolds number for each angular bin (Table 2). The data indicate that the effective magnetic Reynolds number varies for the different angular bins even within the large uncertainties. However, the effective magnetic Reynolds numbers are the same within 2 standard deviations and we find a Reynolds number of approximately $2.5 \cdot 10^6$ fits the tabulated values with this uncertainty. On the basis of this information it is unclear whether the effective magnetic Reynolds number changes at all with the angle relative to the mean magnetic field direction. The uncertainties could be further reduced by adding additional spacecraft pair intervals to the study and that would clarify whether there are meaningful variations of the Reynolds number with angle. The mean effective magnetic Reynolds number from Table 2 is about $12.6 \cdot 10^6$ with a range from 2.0 to $37.0 \cdot 10^6$. Thus all of the present estimates are considerably larger than the values given by *Matthaeus et al.* [2005] ($\sim 2.3 \cdot 10^5$) and *Weygand et al.* [2007] ($\sim 2.6 \pm 0.2 \cdot 10^5$). The difference can be attributed principally to the

significantly smaller values obtained for the Taylor scale in the present study.

[38] *Matthaeus et al.* [2005] fit correlation versus separation with a single exponential. We find that in order to obtain an acceptable fit to the data, we must use two exponentials. The reason why a single exponential does not provide a satisfactory fit is most likely because of the addition of more Cluster data at separations not previously available. From that the double exponential fit we obtain three values: a first decay value (third column of Table 2), a second decay value (fourth column), and a weighting factor (not tabulated). We have assumed that the largest decay value is the correlation scale and can be associated with the largest turbulent eddy scale sizes. However, the physical meaning of the second decay parameter is unclear. The fits to the data indicate that the largest decay value is associated with the largest spacecraft separations (i.e., ACE, Geotail IMP 8, Interball, and Wind) while the smaller decay value is associated with Cluster spacecraft pairs. The most significant difference between these two different sets of spacecraft is that the Cluster spacecraft spend most of their time in the foreshock region. We hypothesize that the second decay parameter may be associated with turbulence within the foreshock region. Table 1 shows that between $20 \cdot 10^3$ km and about $700 \cdot 10^3$ km there are no measurements. In order to determine if the two different decay values are real, then we will need to obtain correlations in that gap. Over the next several years as the THEMIS mission spends more time in the solar wind we will be able to fill some of this gap. Another method to test our hypothesis would be to eliminate Cluster correlation values within the foreshock. However, this would significantly decrease our counting statistics.

4.2. Plasma Sheet

[39] In the plasma sheet, both the correlation scale and the Taylor scale appear to depend on the direction of separation with respect to the mean magnetic field direction. Both scales were longest along the magnetic field and shortest in the perpendicular direction. The plasma sheet itself is anisotropic in its extent. In the Y GSM direction, the plasma sheet extends roughly 25 to 30 R_E and in the Z GSM direction it is typically about 1 to 5 R_E thick at about 19 R_E down the tail. The plasma sheet extent in the X GSM direction is much larger (about 40 to 50 R_E) and the magnetic field is mainly aligned along this direction just above and below the central plasma sheet. Furthermore, Cluster during the summer season crosses the plasma sheet from the north to the south. One may question whether the anisotropy in the plasma sheet turbulence has been imposed by anisotropy in the shape of the plasma sheet. Recognizing that the plasma sheet dimension in the Y GSM direction is considerably larger than the correlation scales and noting that the orbit of the Cluster spacecraft is inclined to 90.7°, one expects that correlations should be insensitive to the orientation of the spacecraft in the $Y Z$ GSM plane. We argue that anisotropy in the plasma sheet turbulence is not the result of the shape of the plasma sheet or the orientation of the separation in the plane perpendicular to the magnetic field. Instead anisotropy may be the result of plasma diffusion. Turbulent plasma can more easily diffuse along the magnetic field direction than across it. *Weygand et al.*

[2005] found that the autocorrelation length of turbulent eddies is longer along the plasma sheet and shorter in the azimuthal and vertical directions. They suggested that these differences mean that the turbulent eddies are ovoid in shape.

[40] The studies of *Weygand et al.* [2005, 2007] found plasma sheet correlation scales between approximately 10,000 km and 20,000 km. *Borovsky et al.* [1997], *Borovsky and Funsten* [2003], and *Neagu et al.* [2002] found the correlation scale to be approximately 10,000 km and about 4,000 km, respectively. The correlation scales in different directions relative to the magnetic field are consistent with those previous works; however, none of those studies used multiple spacecraft to investigate how the correlation scale varies as a function of the angle with respect to the magnetic field direction. *Weygand et al.* [2005] did examine the autocorrelation cutoff times for the different components of the magnetic field in a GSM coordinate system, but they did not look at the autocorrelation cutoff times in a field aligned coordinate system so a direct comparison between their cutoff times and our correlation scale is not meaningful.

[41] Our analysis shows that plasma sheet magnetic turbulence is anisotropic, with correlation scale longer in the parallel direction than in the perpendicular direction. Not only is this the same sense of anisotropy that is found in the solar wind, but, within their mutual uncertainties, the ratio of the two correlation scales in the plasma sheet, 1.78 ± 0.16, is consistent with the ratio we found above for the solar wind and it is almost the same as the value, 1.79 ± 0.36, found by *Osman and Horbury* [2007] in the solar wind. A value of the anisotropy ratio that could be applied to both the plasma sheet and the solar wind and fits within their mutual uncertainties is 1.9. The similarity of the anisotropy in both the plasma sheet and solar wind turbulence may indicate that the two systems are responding to similar mechanisms.

[42] The Taylor scale for the plasma sheet was found to be about 1100 ± 100 km in the perpendicular direction and about 2900 ± 100 km in the parallel direction. In their work on the Taylor scale, *Weygand et al.* [2007] found it to be about 1900 ± 100 km for the plasma sheet, but did not analyze the dependence on direction. The average value of the Taylor scale for all the angular bins in Table 3 is 1800 km and falls within the uncertainty given by *Weygand et al.* [2007].

[43] We found that the plasma sheet Taylor scale is longest along the magnetic field and it is relatively constant for angles between 30° and 90°. As far as we are aware the dependence of the Taylor scale on the magnetic field direction has not been documented previously. Fluctuations at length scales that affect the Taylor scale may possibly link to the anisotropy of the inertial range fluctuations and their interaction with the mean magnetic field [*Oughton and Matthaeus*, 2005], but also could arise from anisotropy of dispersive and dissipative effects, including Landau damping, cyclotron resonance, kinetic Alfven waves and other processes that depend upon the direction of the magnetic field [*Leamon et al.*, 1999; *Gary and Borovsky*, 2004].

[44] Within each interval used for the plasma sheet analysis, the bulk flow speed may vary between zero and several hundred km s^{-1}, attaining even thousands of km s^{-1}
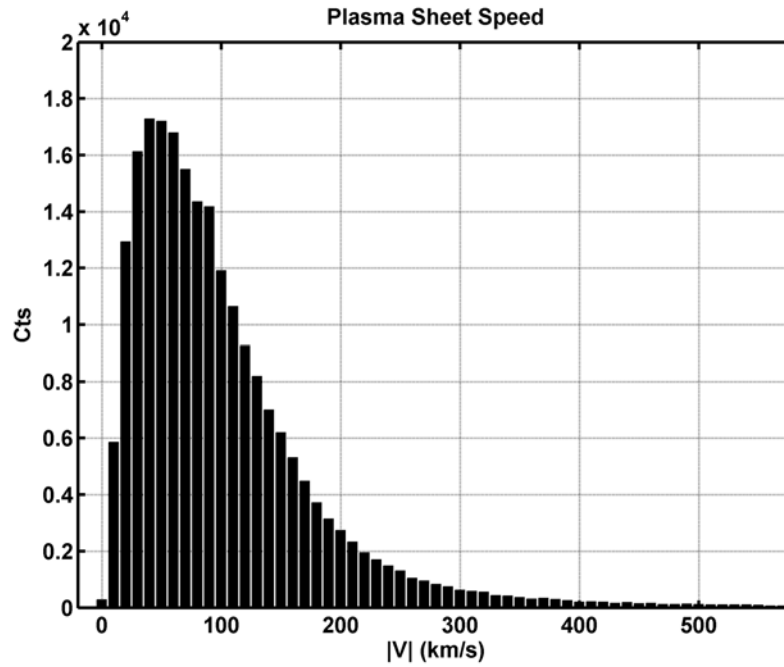
Figure 7. Histogram of the plasma sheet speeds for the intervals used in this study. Bin size is 10 km s^{-1}. Along the y axis are the counts per bin. This plot demonstrates that our turbulence intervals include both very low and very high speed flows.

on rare occasions. The question arises whether the analysis of plasma sheet turbulence is meaningful when intervals of significantly different flow speeds are combined. Solar wind studies suggest that the results obtained from analysis of data using intervals of different flow characteristics [e.g., *Matthaeus et al.*, 1990, 2005] do not differ from those obtained by limiting the data to intervals of slow flow only [*Dasso et al.*, 2005; this paper]. This argument may apply to the inclusion of the high-speed plasma sheet flows, but does not apply to low speeds or speeds of zero. Figure 7 shows the distribution of the plasma sheet speeds for the intervals used in this study. This histogram consists of data from 2001 to 2005. Calibrated CIS data from 2006 to 2007 was not available at the time of this study; however, the uncalibrated CIS data was sufficient to identify the plasma sheet intervals. Figure 7 shows that very low speeds and very high speeds are present in some of plasma sheet intervals. The next question is what speeds are too low to include in our study. The CIS instrument on Cluster is believed to have an uncertainty in speed of about 15 km s^{-1}, which is associated with the determination of the velocity component in the direction along the spin axis of the spacecraft L. M. Kistler, private communication, 2009). We interpret this statement to mean that plasma sheet speeds below 15 km s^{-1} are equivalent to absence of flow. Previous work on the plasma sheet indicates that the nominal speeds are between 30 and 130 km s^{-1} [*Baumjohann et al.*, 1989; *Angelopoulos et al.*, 1993; *Huang and Frank*, 1986, 1987, 1994]. On the basis of the uncertainty in the speed determination and previous plasma sheet work we believe that we can conservatively define speeds less than 30 km s^{-1} as very low.

[45] The definition of what is considered a very high speed flow (i.e., bursty bulk flows) is more problematic

because suggested values vary from study to study ranging from 300 km s^{-1} to 400 km s^{-1} [*Baumjohann et al.*, 1990; *Angelopoulos et al.*, 1994]. For this study we use a relatively conservative estimate of 200 km s^{-1} as the low end of high-speed flows.

[46] An examination of all the 1-h plasma sheet intervals indicates that either low-speed or high-speed flows or both are present for a small fraction of the interval. Figure 8 is a histogram of the duration of intervals with speeds that fall outside the speed band between 30 and 200 km/s. The histogram shows that nearly all of the low- and high-speed flows persist for less than 5 min and most of them last less than tens of seconds. We do not believe that low- or high-speed flow lasting for a few tens of seconds can significantly influence the Taylor scale determination. However, a question that remains is what fraction of a plasma sheet interval with flow speed within the nominal 30 to 200 km s^{-1} range should dictate its retention in the data set analyzed. To address this question we constructed two-dimensional cross-correlation functions for the 30 to 200 km s^{-1} speed range using different fractions to determine which intervals to discard. We found when 80% of the interval corresponds to flows within the 30 to 200 km s^{-1} speed range we are able to get enough cross-correlation points to estimate the Taylor Scale value for most of the angular bins. At fractions larger than 0.8 we do not have enough cross-correlation values to make a reasonable estimate of the Taylor scale.

[47] Table 5 gives the new Taylor scale estimates for the speed range of 30 to 200 km s^{-1}. The Taylor scale value along the mean magnetic field (fifth column, first row) is the same as the Taylor scale estimate in Table 3 within the uncertainty. The Taylor scale estimates in the other angular bins are the same within the uncertainty or no more than
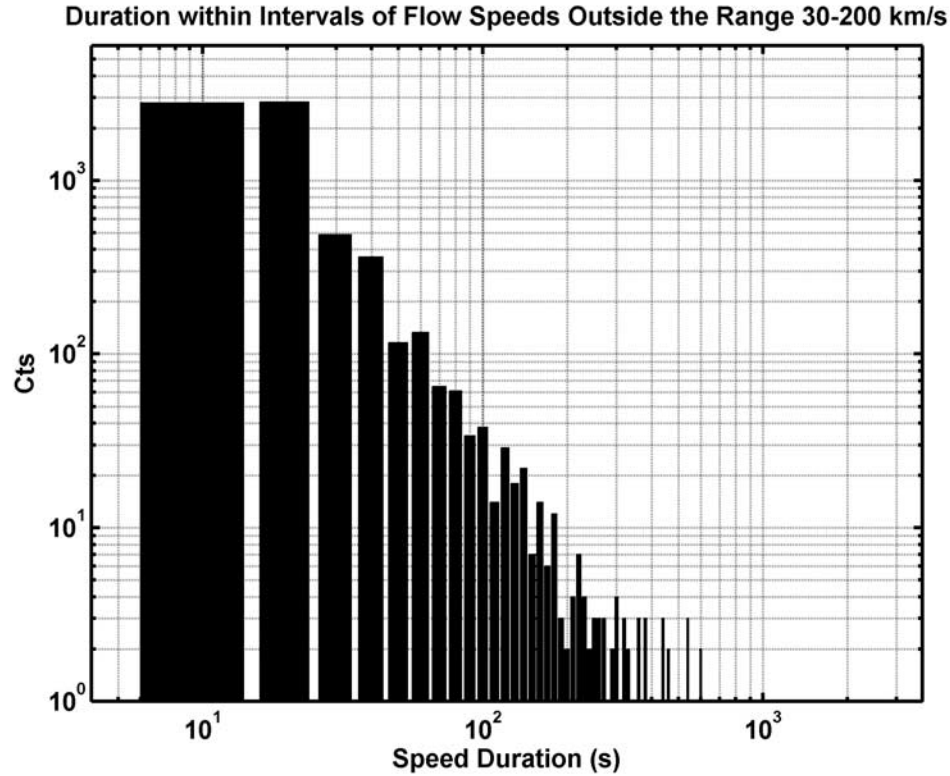
Figure 8. Histogram of the duration of the plasma sheet intervals with flows outside of the speed range 30 to 200 km s[1] in the plasma sheet intervals used in turbulence analysis.

45% larger. Only in the 30° to 40° bin is the Taylor scale for the restricted range of speeds significantly larger than that obtained with our restriction of flow speed, because of the small number of intervals in the angular bin. Also included in Table 5 are the correlation scales previously determined from all the plasma sheet data. We have not estimated new correlation scales for the 30 to 200 km s^{-1} range because cross-correlation values for large spacecraft separations are not available from the 2001 and 2005 data. The largest spacecraft separations occur from 2006 onward but calibrated flow data are not available. Since the Taylor scale values did not change much between the analysis based on all plasma sheet intervals and that based on the subset of limited speed range we do not expect the correlation scale to change significantly. Thus, in the sixth column we have calculated new effective magnetic Reynolds number using the correlation scale from the unrestricted set (third column)

and Taylor scale values from the restricted set (fifth column). These effective magnetic Reynolds numbers are nearly all the same as in Table 3 within the uncertainty. Only in the 30° to 40° bin, for which we do not feel that the Taylor scale estimate is reliable, has the effective magnetic Reynolds number significantly changed.

[48] As an additional test of whether high and low flow speeds and the high flow speeds would modify our results we desired to calculate two-dimensional cross-correlation contours for speeds outside the range, 30 to 200 km s^{-1}. We found that we had insufficient continuous data to get reliable cross-correlation values and hence reliable Taylor scale and correlation scale values for either extremely fast or extremely slow flow conditions.

[49] In the last column of Table 3, the effective magnetic Reynolds numbers in the plasma sheet are calculated from the Taylor and correlation scales. The effective magnetic

Table 5. Plasma Sheet Values of Correlation Scale, Taylor Scale, and Effective Magnetic Reynolds Number for the Various Angular Bins From Magnetic Field Data[a]

Angular Range	Correlation Scale		Taylor Scale		Effective Magnetic Reynolds Number
	Number of Points	λ_{CS} (km)	Number of Points	λ_{TS} (km)	
0° − 30°	114	16400 ± 1000	9	3000 ± 200	30 ± 15
30° − 40°	75	14100 ± 1300	3	2800 ± 100	25 ± 13
40° − 50°	98	14800 ± 1200	9	1700 ± 500	76 ± 66
50° − 60°	114	11100 ± 700	20	1700 ± 400	43 ± 33
60° − 70°	141	10600 ± 700	24	2200 ± 200	23 ± 13
70° − 80°	154	10600 ± 600	21	2400 ± 200	20 ± 10
80° − 90°	153	9200 ± 600	28	1800 ± 100	26 ± 13

[a]The Taylor scale values are determined from the 30 to 200 km s^{-1} speed range, and the correlation scale values are determined using all the plasma sheet data.

Reynolds number varies between 28 and 97 with a mean value of 57. A Reynolds number of 45 fits the values in Table 3 with their uncertainties for all angles. More data intervals are required to improve the statistics in order to more clearly establish whether the Reynolds number varies with the mean magnetic field direction. The effective magnetic Reynolds number found here (45 or 57) is within the range of values (7 to 110) reported by *Weygand et al.* [2007].

5. Summary and Conclusions

[50] In this study we examined in both the solar wind and the plasma sheet the correlation and Taylor scales as functions of the angle of separation relative to the mean magnetic field direction. As far as we are aware this is the first study to use only simultaneous two point correlation measurements to determine the variation of these scales with respect to the mean magnetic field. We find that within the plasma sheet the Taylor scale is longest along the magnetic field ($\sim$2900 $\pm$ 100 km) and shortest perpendicular to the magnetic field ($\sim$1100 $\pm$ 100 km). Finding that the Taylor scale depends on direction in the plasma sheet is puzzling in view of the fact that, to within uncertainty, no directional dependence was identified in the solar wind, but this may involve some elements of anisotropy of dispersive and dissipative effects or may be related to anisotropy at the inertial range scales.

[51] Using the Taylor scale and the correlation scale we derived the effective magnetic Reynolds number for each angular bin. In both the solar wind and the plasma sheet the effective magnetic Reynolds number shows some variability with angle relative to the magnetic field, but remains within 2 standard deviations of a constant value. The uncertainties of our analysis must be reduced by addition of many more events if we are to confirm whether there is an angular variation of the effective magnetic Reynolds number. The value of the magnetic Reynolds number (i.e., Lundqvist number) and its possible anisotropy are important parameters for numerical MHD models.

[52] Our results show that the correlation scale is longest along the magnetic field and shorter perpendicular to the magnetic field in both the solar wind and the plasma sheet. This observation is clearest in the plasma sheet. The ratio of the parallel to the perpendicular correlation scales were found to be 2.62 $\pm$ 0.79 and 1.78 $\pm$ 0.16 for the solar wind and plasma sheet, respectively, almost (within the uncertainty) the same as the value reported by *Osman and Horbury* [2007]. These similar values suggest that not only is the turbulence anisotropic, but the reason for the anisotropy may be the same in the solar wind and the plasma sheet. The fact that the correlation scale varies with respect to the mean magnetic field direction is important to studies of solar and galactic cosmic ray scattering that depend on accurate determination of the perpendicular diffusion coefficient, which is directly proportional to the correlation scale [*Ruffolo et al.*, 2004].

References

Angelopoulos, V., et al. (1993), Characteristics of ion flow in the quiet state of the inner plasma sheet, *Geophys. Res. Lett.*, *20*, 1711–1714.

Angelopoulos, V., C. F. Kennel, F. V. Coroniti, R. Pellat, M. G. Kivelson, R. J. Walker, C. T. Russell, W. Baumjohann, W. C. Feldman, and J. T. Gosling (1994), Statistical characteristics of bursty bulk flow events, *J. Geophys. Res.*, *99*, 21,257–21,280, doi:10.1029/94JA01263.

Balogh, A., et al. (1997), The Cluster magnetic field investigation, *Space Sci. Rev.*, *79*, 65–91, doi:10.1023/A:1004970907748.

Batchelor, G. K. (1970), *Theory of Homogeneous Turbulence*, Cambridge Univ. Press, Cambridge, U. K.

Baumjohann, W., G. Paschmann, and C. A. Cattel (1989), Average plasma properties in the central plasma sheet, *J. Geophys. Res.*, *94*, 6597–6606, doi:10.1029/JA094iA06p06597.

Baumjohann, W., G. Paschmann, and H. Lühr (1990), Characteristics of high-speed ion flows in the plasma sheet, *J. Geophys. Res.*, *95*, 3801–3809, doi:10.1029/JA095iA04p03801.

Bieber, J. W., W. H. Matthaeus, C. W. Smith, W. Wanner, M.-B. Kallenrode, and G. Wibberenz (1994), Proton and electron mean free paths: The Palmer consensus revisited, *Astrophys. J.*, *420*, 294–306, doi:10.1086/173559.

Bieber, J. W., W. Wanner, and W. H. Matthaeus (1996), Dominant two-dimensional solar wind turbulence with implications for cosmic ray transport, *J. Geophys. Res.*, *101*, 2511–2522, doi:10.1029/95JA02588.

Borovsky, J. E., and H. O. Funsten (2003), The MHD turbulence in the Earth's plasma sheet: Dynamics, dissipation, and driving, *J. Geophys. Res.*, *108*(A7), 1284, doi:10.1029/2002JA009625.

Borovsky, J. E., R. C. Elphic, H. O. Funsten, and M. F. Thomsen (1997), The Earth's plasma sheet as a laboratory for turbulence in high-beta MHD, *J. Plasma Phys.*, *57*, 1–34, doi:10.1017/S0022377896005259.

Chuychai, P. J. M., et al. (2009), Technique of measuring and correcting the Taylor microscale, manuscript in preparation.

Crooker, N. U., G. L. Siscoe, C. T. Russell, and E. J. Smith (1982), Factors controlling degree of correlation between ISEE 1 and ISEE 3 interplanetary magnetic field measurements, *J. Geophys. Res.*, *87*, 2224–2230, doi:10.1029/JA087iA04p02224.

Dasso, S., L. J. Milano, W. H. Matthaeus, and C. W. Smith (2005), Anisotropy in fast and slow solar wind fluctuations, *Astrophys. J.*, *635*, L181–L184, doi:10.1086/499559.

Duffy, P., and K. M. Blundell (2005), Cosmic ray transport and acceleration, *Plasma Phys. Controlled Fusion*, *47*, B667, doi:10.1088/0741-3335/47/12B/S49.

Escoubet, C. P., R. Schmidt, and M. L. Goldstein (1997), Cluster-science and mission overview, *Space Sci. Rev.*, *79*, 11–32, doi:10.1023/A:1004923124586.

Gary, S. P., and J. E. Borovsky (2004), Alfvén-cyclotron fluctuations: Linear Vlasov theory, *J. Geophys. Res.*, *109*, A06105, doi:10.1029/2004JA010399.

Gazis, P. R., A. Barnes, J. D. Mihalov, and A. J. Lazarus (1994), Solar wind velocity and temperature in the outer heliosphere, *J. Geophys. Res.*, *99*, 6561–6573, doi:10.1029/93JA03144.

Goldstein, M. L., D. A. Roberts, and C. A. Fitch (1994), Properties of the fluctuating magnetic helicity in the inertial and dissipation ranges of solar-wind turbulence, *J. Geophys. Res.*, *99*, 11,519–11,538, doi:10.1029/94JA00789.

Goldstein, M. L., D. A. Roberts, and W. H. Matthaeus (1995), Magnetohydrodynamic turbulence in the solar wind, *Annu. Rev. Astron. Astrophys.*, *33*, 283–325, doi:10.1146/annurev.aa.33.090195.001435.

Huang, C. Y., and L. A. Frank (1986), A statistical survey of the central plasma sheet: Implications for the substorm models, *Geophys. Res. Lett.*, *13*, 652–655, doi:10.1029/GL013i007p00652.

Huang, C. Y., and L. A. Frank (1987), Reply to Cattell and Elphic, *Geophys. Res. Lett.*, *14*, 776–778, doi:10.1029/GL014i007p00776.

Huang, C. Y., and L. A. Frank (1994), A statistical survey of the central plasma sheet, *J. Geophys. Res.*, *99*, 83–95, doi:10.1029/93JA01894.

Kokubun, S., T. Yamamoto, M. H. Acuna, K. Hayashi, K. Shiokawa, and H. Kawano (1994), The Geotail magnetic field experiment, *J. Geomagn. Geoelectr.*, *46*, 7–21.

Kolmogorov, A. N. (1941), The local structure of turbulence in incompressible viscous fluid for very large Reynolds' numbers, *Dokl. Akad. Nauk SSSR*, *30*, 301–305.

Kraichnan, R. H. (1965), Inertial-range spectrum of hydromagnetic turbulence, *Phys. Fluids*, *8*, 1385, doi:10.1063/1.1761412.

Leamon, R. J., C. W. Smith, N. F. Ness, and H. K. Wong (1999), Dissipation range dynamics: Kinetic Alfvén waves and the importance of β_e, *J. Geophys. Res.*, *104*, 22,331–22,344, doi:10.1029/1999JA900158.

Lepping, R. P., et al. (1995), The WIND magnetic field investigation, *Space Sci. Rev.*, *71*, 207–229, doi:10.1007/BF00751330.

Matthaeus, W. H., M. L. Goldstein, and D. A. Roberts (1990), Evidence for the presence of quasi-two-dimensional nearly incompressible fluctuations in the solar wind, *J. Geophys. Res.*, *95*, 20,673–20,683, doi:10.1029/JA095iA12p20673.

Matthaeus, W. H., S. Dasso, J. M. Weygand, L. J. Milano, C. W. Smith, and M. G. Kivelson (2005), Spatial correlation of the solar wind turbulence from two point measurements, *Phys. Rev. Lett.*, *95*, 231101, doi:10.1103/PhysRevLett.95.231101.

Matthaeus, W. H., J. M. Weygand, P. Chuychai, S. Dasso, C. W. Smith, and M. G. Kivelson (2008), Interplanetary magnetic Taylor scale and implications for plasma dissipation, *Astrophys. J.*, *678*, L141–L144, doi:10.1086/588525.

Milano, L. J., W. H. Matthaeus, P. Dmitruk, and D. C. Montgomery (2001), Local anisotropy in incompressible magnetohydrodynamic turbulence, *Phys. Plasmas*, *8*, 2673–2681.

Neagu, E., J. E. Borovsky, M. F. Thomsen, S. P. Gary, W. Baumjohann, and R. A. Treumann (2002), Statistical survey of magnetic field and ion velocity fluctuations in the near-Earth plasma sheet: Active Magnetospheric Particle Trace Explorers/Ion Release Module (AMPTE/IRM) measurements, *J. Geophys. Res.*, *107*(A7), 1098, doi:10.1029/2001JA000318.

Nozdrachev, M. N., et al. (1995), Magnetic field measurements onboard the INTERBALL TAIL spacecraft: The FM-3I instrument, in *INTERBALL: Mission and Payload*, pp. 228–229, Cent. Natl. d'Etudes Spatiales, Paris.

Osman, K. R., and T. S. Horbury (2007), Multispacecraft measurement of anisotropic correlation functions in the solar wind turbulence, *Astrophys. J.*, *654*, L103–L106, doi:10.1086/510906.

Oughton, S., and W. H. Matthaeus (2005), Parallel and perpendicular cascades in solar wind turbulence, *Nonlinear Processes Geophys.*, *12*, 299–310.

Rème, H., et al. (1997), The Cluster ion spectrometry (CIS) experiment, *Space Sci. Rev.*, *79*, 303–350, doi:10.1023/A:1004929816409.

Richardson, J. D., K. L. Paularena, A. J. Lazarus, and J. W. Belcher (1995), Radial evolution of the solar wind from IMP 8 to Voyager 2, *Geophys. Res. Lett.*, *22*, 325–328, doi:10.1029/94GL03273.

Roberts, D. A., M. L. Goldstein, L. W. Klein, and W. H. Matthaeus (1987), Origin and evolution of fluctuations in the solar wind: Helios observations and Helios-Voyager comparisons, *J. Geophys. Res.*, *92*, 12,023–12,035, doi:10.1029/JA092iA11p12023.

Ruffolo, D. W., H. Matthaeus, and P. Cuychai (2004), Separation of magnetic field lines in two-component turbulence, *Astrophys. J.*, *614*, 420–434, doi:10.1086/423412.

Smith, C. W., N. S. Ness, M. Acuña, L. F. Burlaga, J. L'Heureux, and J. Scheifele (1998), The ACE magnetic fields experiment, *Space Sci. Rev.*, *86*, 613–632.

Smith, C. W., W. H. Matthaeus, G. P. Zank, N. F. Ness, S. Oughton, and J. D. Richardson (2001), Heating of the low-latitude solar wind by dissipation of turbulent magnetic fluctuations, *J. Geophys. Res.*, *106*, 8253–8272, doi:10.1029/2000JA000366.

Taylor, G. I. (1938), The spectrum of turbulence, *Proc. R. Soc. London, Ser. A*, *164*, 476–490, doi:10.1098/rspa.1938.0032.

Tu, C. Y., and E. Marsch (1995), MHD structures, waves and turbulence in the solar wind, *Space Sci. Rev.*, *73*, 1–210, doi:10.1007/BF00748891.

Velli, M. (2003), MHD turbulence and the heating of astrophysical plasma, *Plasma Phys. Controlled Fusion*, *45*, A205–A216, doi:10.1088/0741-3335/45/12A/014.

Weygand, J. M., et al. (2005), Plasma sheet turbulence observed by Cluster II, *J. Geophys. Res.*, *110*, A01205, doi:10.1029/2004JA010581.

Weygand, J. M., M. G. Kivelson, K. K. Khurana, H. K. Schwarzl, R. J. Walker, A. Balogh, L. M. Kistler, and M. L. Goldstein (2006), Non-self-similar scaling of plasma sheet and solar wind probability distribution functions of magnetic field fluctuations, *J. Geophys. Res.*, *111*, A11209, doi:10.1029/2006JA011820.

Weygand, J. M., W. H. Matthaeus, S. Dasso, M. G. Kivelson, and R. J. Walker (2007), Taylor scale and effective magnetic Reynolds number determination from the plasma sheet and the solar wind magnetic field fluctuations, *J. Geophys. Res.*, *112*, A10201, doi:10.1029/2007JA012486.

Williams, L. L., G. P. Zank, and W. H. Matthaeus (1995), Dissipation of pickup-induced waves: A solar wind temperature increase in the outer heliosphere?, *J. Geophys. Res.*, *100*, 17,059–17,067, doi:10.1029/95JA01261.

————————————

S. Dasso, Instituto de Astronomía y Física del Espacio, Facultad de Ciencias Exactas y Naturales, Universidad de Buenos Aires, 1428 Buenos Aires, Argentina.

L. M. Kistler and C. Mouikis, Experimental Space Plasma Group, University of New Hampshire, Durham, NH 03824, USA.

M. G. Kivelson and J. M. Weygand, Institute of Geophysics and Planetary Physics, University of California, 3845 Slichter Hall, P.O. Box 951567, Los Angeles, CA 90095-1567, USA. (jweygand@igpp.ucla.edu)

W. H. Matthaeus, Bartol Research Institute, Department of Physics and Astronomy, University of Delaware, 217 Sharp Laboratory, Newark, DE 19716, USA.